DOI: 10.13009/EUCASS2019-603

Relationship between metallographic observation, tensile and yield strength in 7449 aluminium alloy thick plates

J.A.Heredero, J.M.Antoranz, J.M.Badia, M.J.Viscasillas, E.Andres*
Materiales y producción Aeroespacial. Escuela Técnica Superior de Ingeniería Aeronaútica y del Espacio. Universidad Politécnica de Madrid
**Corresponding author: email: joseantonio.heredero@upm.es*

Abstract
7449 Aluminium alloy is a recent development of the heat treatable commercial wrought alloys with high Zn and Mg contents. Tensile and yield (0.2%) strength have been measured through thickness of 54 mm thick plate, in the as-received condition (T7651) and for another heat treatments like peak aged treatment, interrupted heat treatment and one treatment with a high over aged condition. It has been found one abnormal evolution of these mechanical properties. This work attempts to explain this abnormal variation through metallography observation. Optical microscope, Scanning Electron Microscope (SEM) and Energy Dispersion Spectroscopy (EDS) techniques have been used.

Keywords: 7449 aluminium alloy, SEM, EDS, heat treatment, tensile strength, yield strength

1. Introduction

Aluminium alloy industry has been developed in parallel to the aircraft industry. Apart from safety, which must always be present in the aircraft design principles, another very important driving force for airlines companies is the reduction of the aircraft operation cost. Taking into account this assumption, the correct choice of aluminium alloy plays a fundamental role. For example, by selecting a very high strength aluminium alloy, the aircraft weight is reduced and as a consequence, fuel consumption is improved, and payload and range are increased [1].
In general, aluminium alloys have been used as the primary structure, due to their well-known performance characteristics, and low weight. This is the main reason that aluminium alloys have been present in commercial aircraft for almost a century [2]. In addition, during the recent years, most of the new material developments, have also been focused on several types of aluminium alloys.
It is within the 7XXX series of wrought aluminium that most of the developments have occurred [3]. 7XXX series of aluminium wrought alloys, are characterized for having higher mechanical strength in comparison with other classes of aluminium alloys. Specially, it is particularly noteworthy that, 7XXX series of aluminium, having weight Zn contents equal to or greater than 8.4%, like Aluminium Alloy (AA)7055 and AA 7449, provides the high strength, that have been required during the last decade for upper wing skin materials for commercial aircraft [4].
For high strength 7XXX series of wrought aluminium, important mechanical properties like, strength, ductility, modulus, corrosion resistance, fracture toughness and fatigue resistance are demanded. This is in line with the development of the modern aerospace industry and the change of the traditional aircraft design concepts [5]. Most of these properties can be controlled by appropriate alloying, processing, heat treatments and correct combinations of these [6].
Due to continuous improvement of the mechanical properties of aerospace aluminium alloys, a series of high strength 7XXX wrought aluminium alloys have been developed. Example of these alloys are 7075, 7150, 7055 and 7449 shown in chronological order [1].
Focusing on the 7449 wrought aluminium alloy, it is a recent evolution of the 7000 series alloys firstly used towards the end of the Second World War. 7449 was developed by Pechiney in France during 1990s. It was designated as a high strength plate material with low quench sensitivity and primary used in the aerospace industry for medium and thick sections (thickness ≤ 100 mm) [7] [8].
Wrought AA7449 is a precipitation hardenable Al-Zn-Mg-Cu alloy, with a Zn content by weight in the range 7.5%-8.7%. It is supplied normally in two commercial over-aged heat treatments: T7651 (over-aged) used for example in A380 aircraft ribs and T7951 (slightly over-aged) used for example in A380 aircraft upper wing ribs [9], [10], [11]. The designation Txx51 means that significant stress relief treatment, by stretching, has been applied immediately after quenching.

Copyright © 2019 by J.A. Heredero and J.M. Antoranz. Published by the EUCASS association with permission.

DOI: 10.13009/EUCASS2019-603

Although stress relief treatment has been applied by stretching in the as-received condition, as it is a thick plate (54mm thickness), properties like tensile and yield (0.2%) strength can be evaluated through the thickness.
As a result of this evaluation, abnormal evolution in the values of these mechanical properties has been found. Tensile and yield strength are higher in the centre of the plate than near of the surface. This abnormal behaviour has been detected in the as-received condition (T7651), and in several heat treatments performed in this work. Heat treatments like peak aged, interrupted treatment or even one treatment with high over aged condition, show an abnormal variation of the tensile and yield strength though the thickness. See table 3 for more details.
In order to try to explain these abnormal variations of the mechanical properties, metallography structure examination is shaping up as the best way. Through metallography analysis it is possible to quantify the effects of different fabrication processes, heat treatments or new procedures and even to analyse the root cause of failures [12] [13]. In addition, mechanical properties and the general behaviour of a wrought aluminium alloy is intimately linked to its casting, homogenization, preheat, hot or cold reduction, annealing, solution treatment and the type of precipitation structure [13].
In general, for 7XXX series of wrought aluminium alloys, several particles can be distinguished [6], [12], [14], [15], [16]:

- **Coarse particles**. They are particles whose size ranges from 0.1 μm to 10 μm, constituted by Fe and Si which are always present as impurity elements. They may be either intermetallic compounds or metallic crystals formed during solidification. Also, it is included in this definition solid phase separated first from the melt. This is the case of macroscopically large and undesirable particles of Al_7Cr, Al_3Ti, Al_3Zr, formed by a peritectic reaction when chemical composition is not closely controlled. In general, they are not beneficial. These particles are not appreciably dissolved during subsequent thermomechanical processing and heat treatments. They are considered as large particles with irregular shape, which can be resolved by light microscope.
- **Dispersoids.** They are particles whose size ranges from 0.05 μm to 0.5 μm. They are typically constituted by Cr, Mn, Ti and Zr. These particles are formed during the homogenization phase. For example, Cr is precipitated from supersaturated solution heavily concentrated in the primary dendrite regions. The size distribution of dispersoids is a key factor of controlling degree of recrystallization, recrystallized grain size and crystallography texture. The dispersoids inhibit recrystallization and faster formation of the fine subgrain structure. Three factors affect quantity and size of the dispersoids: composition, heat history and mechanical deformation. 7xxx wrought aluminium alloys that contain Zr (newer aluminium alloys), form coherent Al_3Zr dispersoids instead of the older aluminium alloys which forms incoherent dispersoids. Taking into account that nucleation is difficult on coherent interfaces, the aluminium alloys with Zr are less quench sensitive than incoherent ones. On the contrary, 7xxx aluminium wrought alloys with Cr and Mn dispersoids exhibit incoherent interface. This incoherent interface serves to nucleate $MgZn_2$. Similar to the above constituents' particles, dispersoids are not modified during the heat treatments.
- **Precipitates** with size from 0.01 μm to 0.1 μm. They are formed during any heat operation below solvus temperature. The main feature of the fines precipitates is the hardening effect, but coarse precipitates do not contribute to age hardening. In addition, coarse precipitates reduce properties such as ductility, fracture toughness and resistance to intergranular corrosion. Precipitates nucleate and grow during artificial and natural aging at subgrain and grain boundaries and at the particle – matrix interfaces. They can be spherical, needles, laths, plates, among other shapes. Such small sizes can only be resolved by SEM and TEM microscope.

One sketch which relates the microstructure of the particles described above, with the different processing steps and mechanical properties for one aluminium wrought alloy can be found in [17].

Taking into account all above considerations, the aim of this work is to explain the abnormal behaviour of tensile and yield strength through the thickness. In order to do this, one deep metallographic analysis of 7449 in the as-received T7651 condition, has been performed.
Grain deformed structure, observed by optical microscope, shows more deformed structure in the external surface of the plate than in the centre surface of the plate. This is a typical grain deformed shape structure, obtained after rolling operations.
Metallographic structure, inspected by scanning electron microscope (SEM), shows two different kinds of intermetallic particles: one in bright colour and other in dark colour.
Finally, EDS semiquantitative microanalysis, shows no chemical segregation of the fundamental composition, through the plate thickness. In addition, EDS has allowed to characterize two types of the intermetallic particles with bright and dark colour observed by SEM, and present in the microstructure. Bright colour particles are probably coarse particles according to above explanation, which are not modified during subsequent heat treatments such as quenching and aging.
Optical and SEM metallography examination, and EDS analysis have been performed at samples extracted from longitudinal L direction and examined through the plate's thickness.

DOI: 10.13009/EUCASS2019-603

2. Experimental procedure.

Chemical composition of the 7449 alloy, investigated in the present work, is shown in the table 1.

Table 1. Chemical composition of 7449 experimental alloy (wt %)

Zn	Mg	Cu	Mn	Fe	Si	Ni	Zr	Cr	Ti	Al
8.40	2.10	1.80	0.05	0.06	0.03	0.001	0.11	0.055	0.02	87.37

Wrought Aluminium alloy (AA) 7449 was supplied by "PREMASA Formatos aeronaúticos S:A" in T7651 heat treatment condition and in the form of plate with the following dimensions: 1560 mm (L-longitudinal) x 765 mm (LT-Long transverse) x 54 mm (ST-short transverse). The plate was cut in six equals blocks with the dimensions 220mm (L) x 765 mm (LT) x 54 (ST) mm and one extra block with the dimensions 210 mm (L) x 765 mm (LT) x 54 mm (ST) according to the sketch of the figure 1.

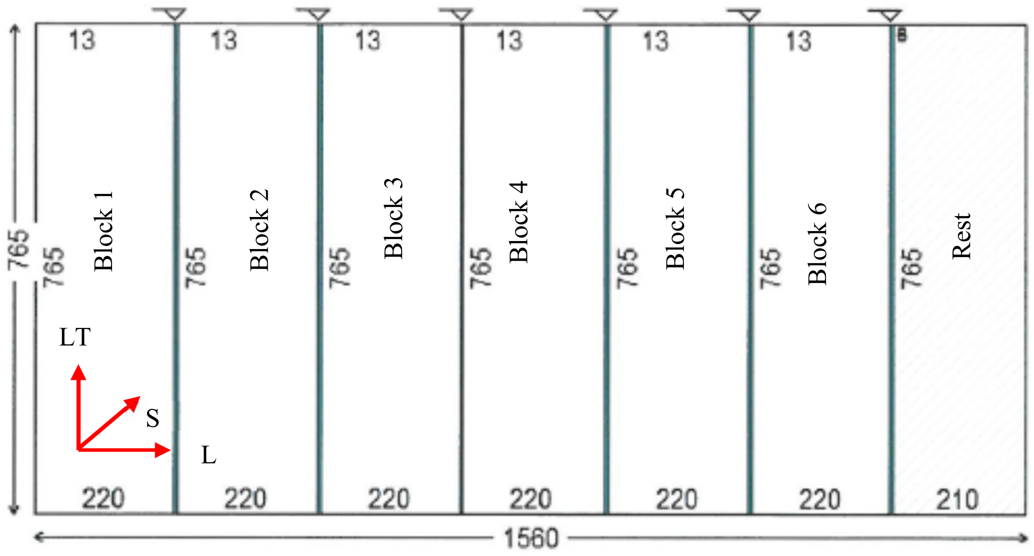

Figure 1. Sketch of the plate in as received condition supplied by PREMASA with the main directions.

One block is shown in the following figure 2 as an example:

Figure 2. Example of the block for to work

For high strength Al-Zn-Mg-Cu thick plates, like for example the as-received Aluminium Alloy (AA)7449 T7651 used in this work, the processing involves several sequences of steps in the following order [6], [9]:

- Casting
- Homogenisation

DOI: 10.13009/EUCASS2019-603

- Hot rolling
- Solution treatment, followed by quenching
- Stress relief by stretching
- and finally, artificial age hardening

The studied AA 7449 in-the as received condition, T7651, has been performed with the following last steps:
- Solution treated
- Controlled stretched
- Artificially aged

Several heat treatments have been performed during this work. Among them, it is worth highlighting the following presented in the table 2.

Table 2: Heat treatments applied to the 7449 Aluminium Alloy

Heat treatment denomination	**Description**
T7651 (as received condition)	Proprietary artificial aging, more overaged
TT3	Solution+ 100 ºC for 6 hours +135ºC for 12 hours
TT6 (peak aged)	Solution + 120ºC for 24 hours
TT7	Solution+ 150ºC for 6 hours + 95ºC for 24 hours
TT9	Solution + 120ºC for 3 hours+60ºC for 72 Hours + 90ºC for 24 hours
TT10 (high over aged)	T7651+ 160ºC for 8 hours
T6I6 interrupted aging treatment [a]	Solution +120ºC for 6 hours+ cold water quenched + 65ºC for 192 hours +120ºC for 150 hours

[a] T6I6 this heat treatment is called interrupted (I) heat treatment. The denomination T6IX involves a novel treatment wherein artificial aging at a typical T6 aging temperature, is interrupted (I) by holding the alloy at a reduced temperature for a prolonged period of time. Afterwards aging is allowed to continue at reduced temperature, for example room temperature (T6I4) or at temperature close to conventional T6 heat treatment (T6I6) [18], [19].

All heat treatments performed in this work have been solution heated to 468ºC for 3 hours in salt bath REVSAL 430 followed by water quenching to the room temperature. This first step was performed in electrical resistance vertical furnace. Artificial aging steps were carried out by heater HERAEUS UT6120 provided by air forced circulation.
In order to perform metallographic analysis, the specimen was extracted from the block by mechanical saw. The inspected face corresponds to L direction, according to figure 3.

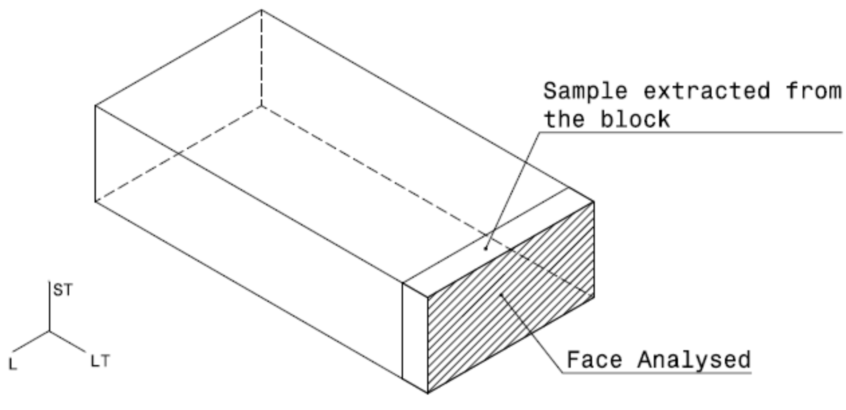

Figure 3. Sketch of the sample extracted from the block and the face analysed in the microscope.

The sample used for the metallography study by optical microscope and SEM was mechanically grinded and polished and then polished by colloidal silica. Finally, the sample used for the optical microscope observation was etched by Keller’s reagent.

DOI: 10.13009/EUCASS2019-603

Sample was observed with an optical microscope LEICA MZ.8, and REITCHER. For SEM, the observation has been carried out with a HITACHI S-3400N microscope.
For tensile test, specimens were extracted in L direction. Four cylindrical specimens were extracted through the thickness (ST direction), with total length l=155 mm and diameter d=8 mm. Two specimens were extracted near the surface (specimens #1 and #4) and the other two in the centre of the plate (specimens #2 and #3), according to figure 4. Tensile test was performed with a universal testing machine MTS, and according to [20] standard.

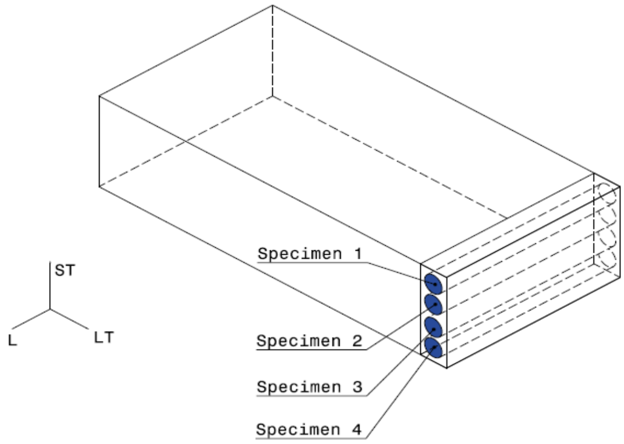

Figure 4. Sketch of the specimens extracted to perform tensile test.

The evaluation of the amount and percentage of microstructure particles has been performed by free software ImageJ.

3. Results and discussion

3.1 Strength results

Tensile strength, yield strength (0.2%) and elongation to fracture, have been measured for the heat treatments described in table 2. The results are shown in table 3

Table 3. Tensile, yield (0.2%) strength and elongation to fracture results

Heat treatment denomination	Tensile strength (MPa)		Yield strength (0.2%) (MPa)		Elongation to fracture (%)	
	Centre [a]	External [b]	Centre [a]	External [b]	Centre [a]	External [b]
T7651 (as received condition)	602	555	566	535	12.2	12.5
TT3	654	596	603	536	10.9	14.4
TT6 (peak aged)	632	561	567	494	11.5	17.8
TT7	646	603	624	562	12.8	15.8
TT9	620	560	539	477	10.6	15.9
TT10 (high over aged)	543	521	498	485	12.2	14.5
T6I6 interrupted aging treatment	651	594	627	562	16.8	16.3

[a] It is the average values of tensile, yield strength and elongation to fracture of the specimens #2 and #3 according to figure 6.
[b] It is the average values of tensile, yield strength and elongation to fracture of the specimens #1 and #4 according to figure 6.

According to table 3, both tensile and yield strength values are higher for the specimen extracted from the centre of the plate that for specimen extracted near the surface. This is an abnormal distribution profile, because the opposite is expected: tensile and yield strength to be higher near the surface than in the centre of the plate, since the intensity of the rolling operation is expected to have been higher near the surface that in the centre of the plate. Elongation to

DOI: 10.13009/EUCASS2019-603

fracture values are higher in the external than in the centre of the plate. There is an exception for interrupted aging treatments.
The values of hardness and electric conductivity, taken as average measurements through thickness of plate, are shown in table 4.

Table 4. Hardness and electric conductivity: average values through the thickness

Heat treatment denomination	**Hardness (HV30)**	**Electric conductivity (MS/m)**
T7651 (as received condition)	171	22,50
TT3	205	17,91
TT6 (peak aged)	195	19,99
TT7	206	19,10
TT9	194	16,97
TT10 (high over aged)	170	22,63
T6I6 interrupted aging treatment	199	19,64

Note that for example in the as-received condition, hardness is higher near the surface than in the centre of the plate (6% in average). Hardness evolution is contrary to tensile and yield strength evolution. This is an expected evolution according to the intensity of the rolling operation. On the other hand, electric conductivity is higher in the centre of the plate than near the surface (2.5% in average).

In order to try to explain these abnormal values measured of tensile and yield strength, a deep metallography analysis has been launched.

3.2 Metallographic observation

Figures 5 to 7 show optical micrographs, of the as-received condition T7651 in the three metallurgical directions (respectively longitudinal L, transversal T and short S) and in the same position through the thickness. It can be highlighted that grain structure in T direction is very similar to the grain structure in L direction.
The figures show how the rolling operations generate a deformed and elongated grain in the L direction that also generate anisotropy. This is a typical microstructure of a rolled and heat-treated component which it is in accordance with [9], [14] and [23].

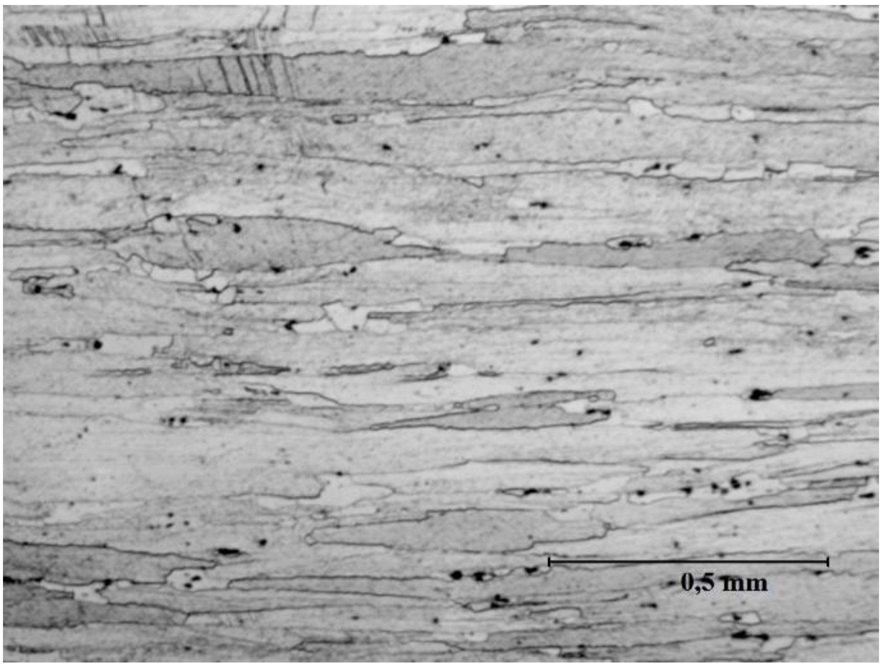

Figure 5. Optical micrograph showing the structure in L direction for the T7651

DOI: 10.13009/EUCASS2019-603

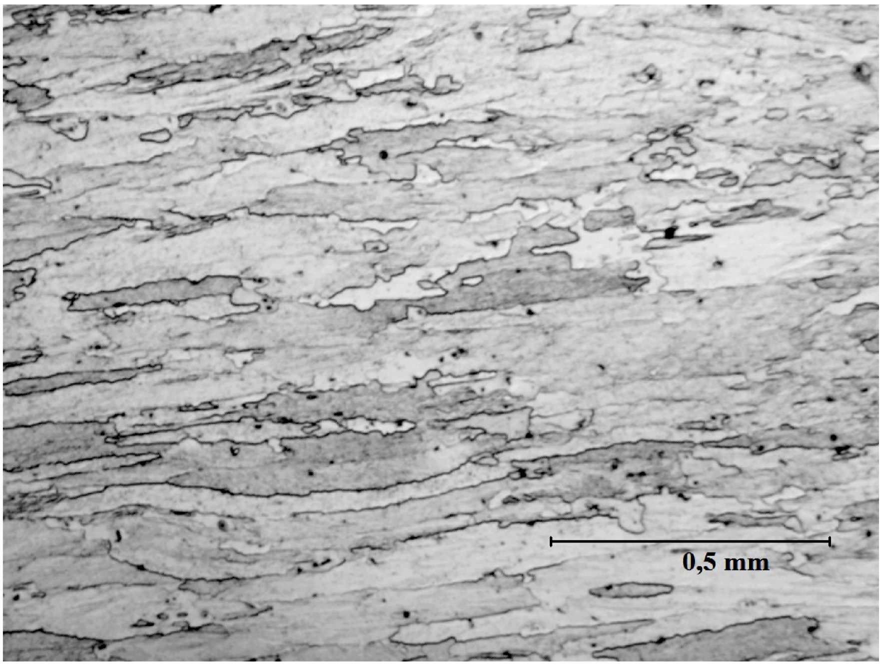

Figure 6. Optical micrograph showing the structure in T direction for the T7651

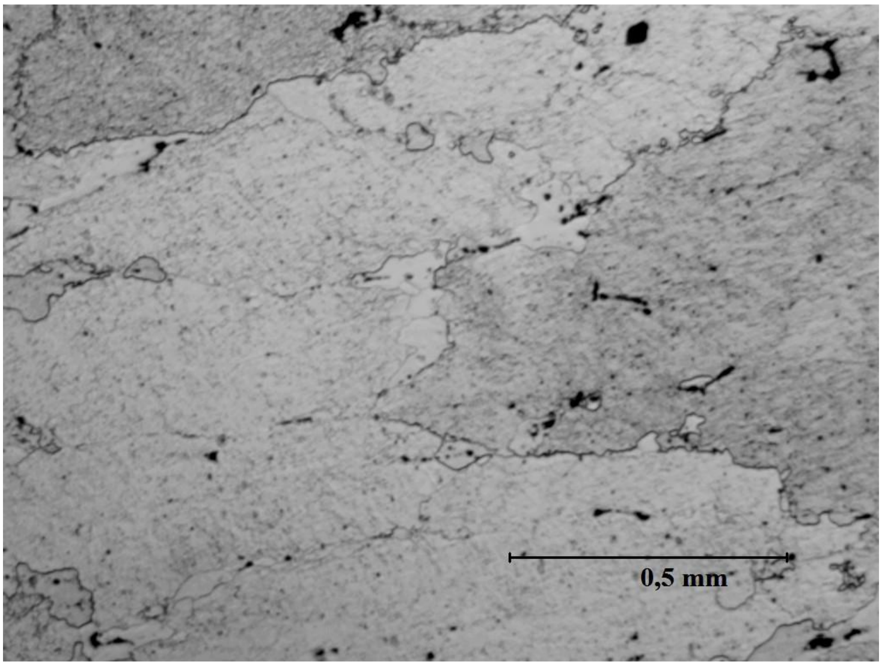

Figure 7. Optical micrograph showing the structure in S direction for the T7651

Once the grain structure has been characterized in the three metallurgical directions, the detailed examination of the metallographic structure will be focused in L direction and through the thickness. In order to do this, the recommendations given in [12] and [13] have been followed. As it is reported in [12] and [13], as a general rule to perform the metallography observation, the examination should be started with low magnification, like normal vision level, and continues with higher magnification, for example scanning electron microscope (SEM). Taking into account this rule, the metallographic examination of this work has been performed at the first with optical microscope and following with scanning electron microscope (SEM) and energy dispersion spectroscopy (EDS).

DOI: 10.13009/EUCASS2019-603

3.2.1 Observation by optical microscope

For the sample extracted from the block according to previous figure 3, observation by optical microscope has been performed in the as received condition T7651.
Optical microscope observation has been carried out, at the first step, with low magnification (figures 8 and 10) and second step with high magnification (figures 9 and 11). Figures 8 and 9 have been extracted near the surface of the plate and figures 10 and 11have been extracted at the centre of the plate.

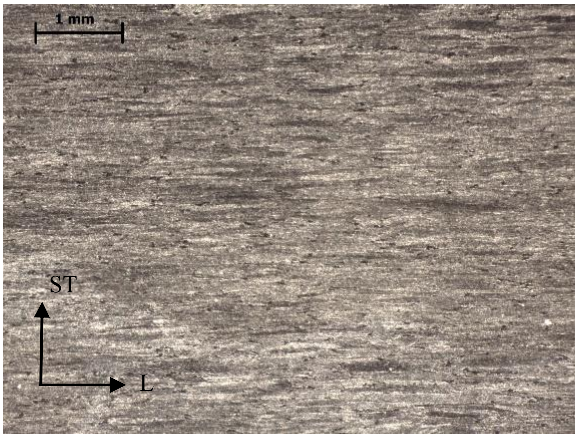

Figure 8. Grain structure, in L direction, of the area near to surface of the plate.

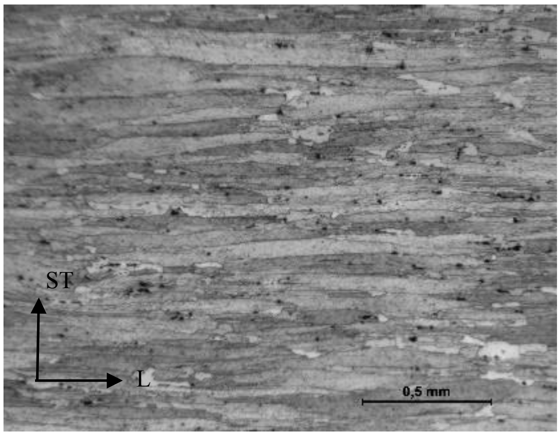

Figure 9. Grain structure, in L direction, of the area near the surface of the plate.

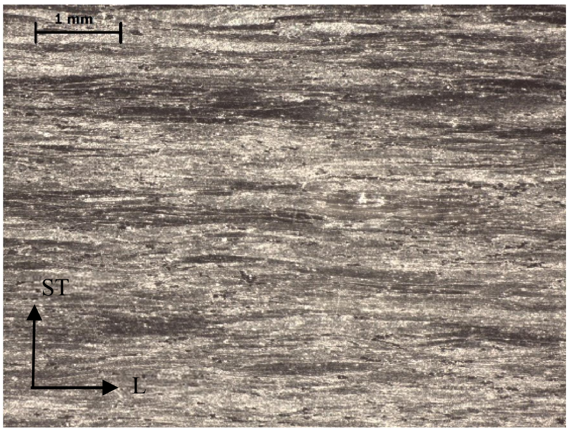

Figure 10. Grain structure, in L direction, of the centre of the plate.

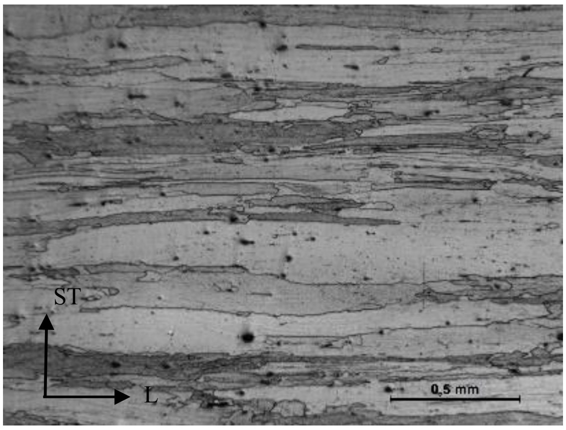

Figure 11. Grain structure, in L direction, of the centre of the plate.

General observation of the above figures shows one enlarged grain structure in the L direction which corresponds to the direction of the main stress applied in service.
According to the above figures 8 and 9, in the area near the surface, it can be appreciated one grain structure composed by thinner and more elongated grains than in the centre of the plate(figures 10 and 11), where the grain is thicker.
As it is reported in [9], in the rolling direction the grain structure is composed by a mixture of small subgrains, large grains generated by recrystallization at hot temperature and elongated grains due to rolling operation.
In this situation, although in figure 9 it can be appreciated that the area near the surface of the plate has the structure more developed than the corresponding one of the centre area, figure 11, near the surface of the plate there is one incipient recrystallization, which is not appreciate in the centre. This is due to the fact that the rolling operation intensity has not been the same through the thickness (ST) direction due to the thick plate, being higher near the surface than in the middle.

DOI: 10.13009/EUCASS2019-603

The small amount of recrystallization could be due to the dispersoids particles inhibiting the movements of both dislocation cell boundaries and grain boundaries. Due to the pinning effects of dispersoids, a whole recrystallisation has not been completed because there was not enough internal energy stored during the rolling operation [6].
It is important to highlight that from a fracture toughness point of view, it desirable to minimise the degree of recrystallisation [6]. In order to do this, during the solution treatment, time and temperature should be kept as low as possible, but achieving at the same time, the maximum dissolution of soluble particles for to maximize strength properties and corrosion resistance [21], [22].

3.2.2 Observation by SEM and EDS

The specimen extracted from the block, according to figure 3 has also been observed by SEM and EDS. The observation has been carried out through the thickness (ST). Particularly one area near the surface of the plate and other area at the centre of the plate have been considered. For each of these areas, eight different locations, in L direction, have been considered. Figures 12 and 13 show two random locations in each area.

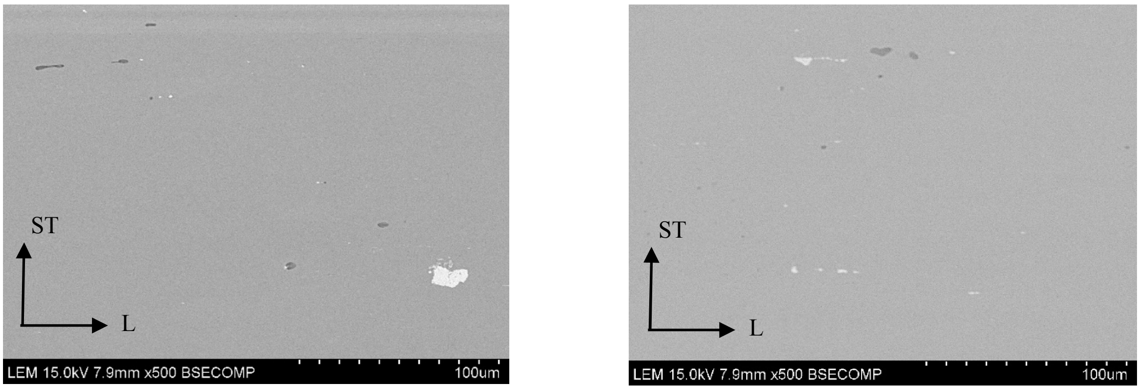

Figure 12. SEM observation corresponding to two different locations of the centre of the plate in L direction.

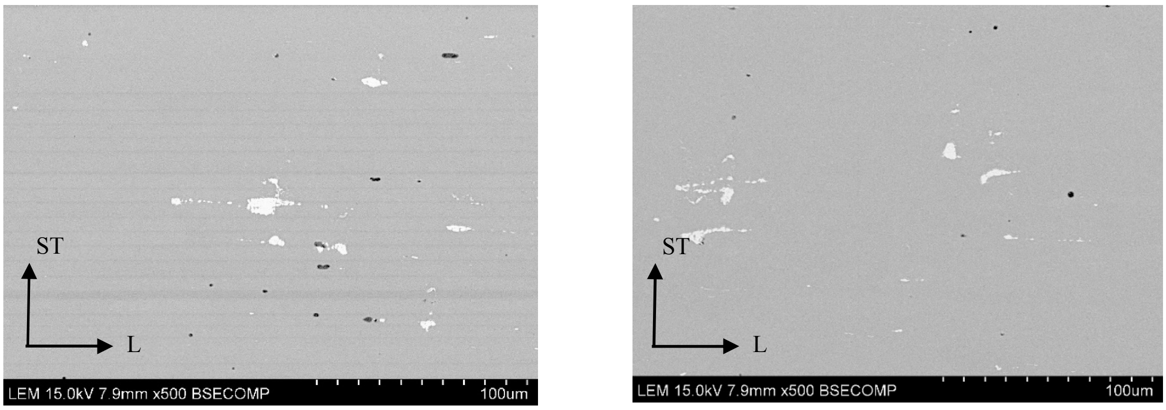

Figure 13. SEM observation corresponding to two different locations of the area near the surface of the plate in L direction.

In these SEM micrographs, two different kinds of particles can be observed: intermetallic particles of bright colour and other dark coloured ones. In general, bright particles are more polygonal and fragmented than dark particles, which are more rounded. In addition, bright particles are larger than the dark ones. See also figures 20 and 21. This typology and morphology of particles has been found for example in [23], [24], [25] for 7050 Aluminium Alloy (AA).
In order to quantify the percentage of area occupied by both kinds of particles, at the centre of the plate and near the surface of the plate, the eight fields of observation, mentioned at the beginning of this section, have been considered. In all of them, there is a greater number of total intermetallic particles (bright and dark) in the area near the surface than in the centre of the plate, see figures 14 and 15. There is also a greater number of bright particles than dark ones,

DOI: 10.13009/EUCASS2019-603

for both the centre and near the surface of the plate, see figures 16 and 17. In the following graphs, the percentage of area taken up by intermetallic particles with respect to the total area of the micrograph is plotted.

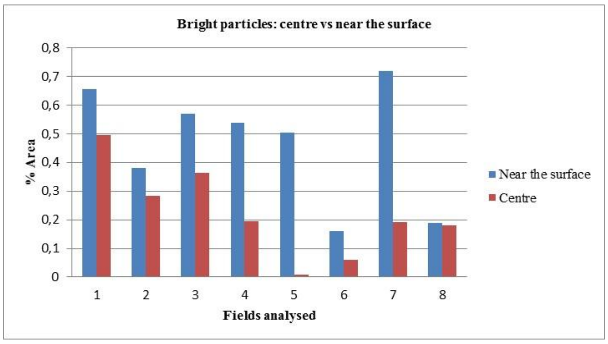

Figure 14. Percentage of the area taken up by bright particles in the centre vs near the surface of the plate

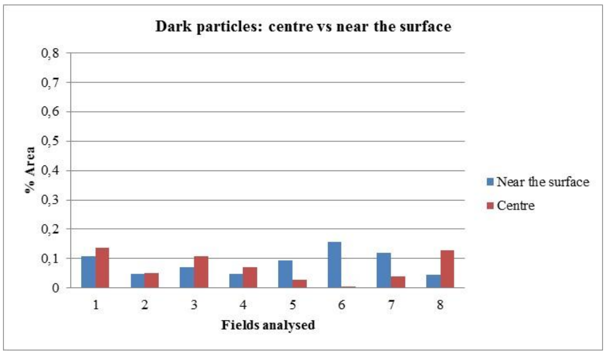

Figure 15. Percentage of the are taken up by dark particles in the centre vs near the surface of the plate

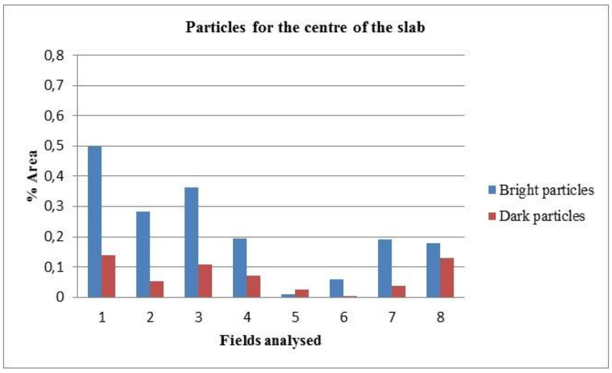

Figure 16. Percentage of the area taken up by bright and dark particles for the centre of the plate

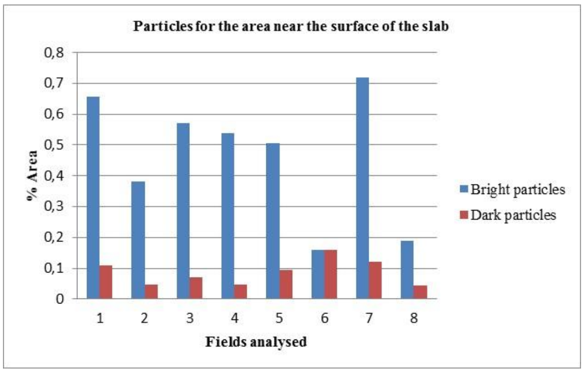

Figure 17. Percentage of the area taken up by bright and dark particles for the area near the surface of the plate

EDS semi quantitative micro-analysis has also been performed in order to identify the chemical composition of the fundamental elements present in the alloy and of the bright and dark intermetallic particles.
Regarding the chemical composition of the fundamental elements present in the alloy, the EDS spectrums for the centre and for the area near the surface are shown in the figures 18 and 19.

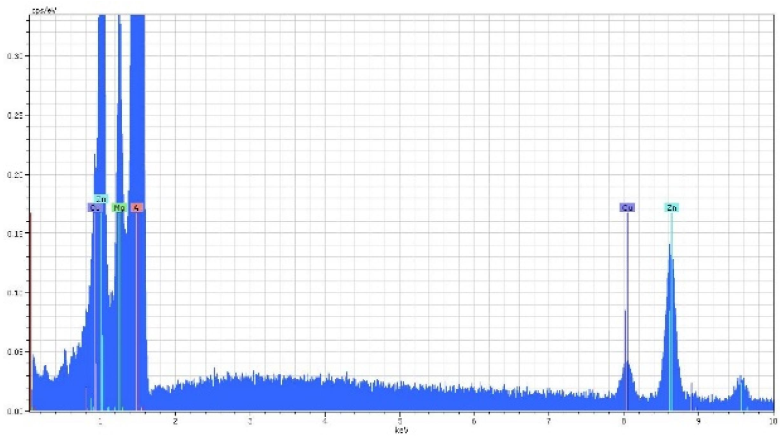

Figure 18. EDS spectrum of centre

DOI: 10.13009/EUCASS2019-603

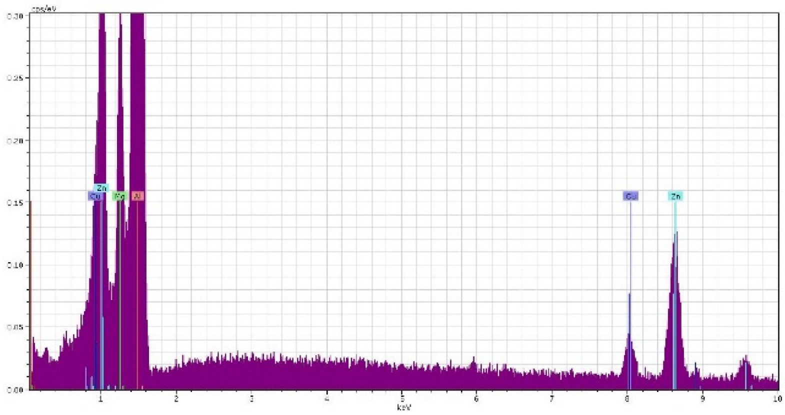

Figure 19. EDS spectrum of area near the surface

Table 5 shows the chemical composition, in weight percentage, of the above EDS spectrums

Table 5: EDS spectrums for the centre and near the surface of the plate

Location	**Weight %**			
	Al	**Zn**	**Mg**	**Cu**
Centre	86.6	8.4	3.2	1.9
Near surface	86.4	8.5	3.2	2.0

According to the values shown above in table 5, the main conclusion is that there is not chemical segregation through the thickness.
The main reason to explain this, could be that according to the sequence of steps for Al-Zn-Mg-Cu thick plates described in [6] and [9], homogenisation step has removed the micro and macro segregations present after casting operations, leading to homogeneous chemical composition. As it is reported in [6] one of the main purposes of the homogenisation of the 7xxx series alloys, is to reduce the micro-scale segregation formed during casting operation.
On the other hand, EDS analysis has been used in order to identify the chemical composition of the intermetallic particles. Figure 20 shows detailed SEM micrograph of the bright and dark intermetallic particles, located on the area near the surface.

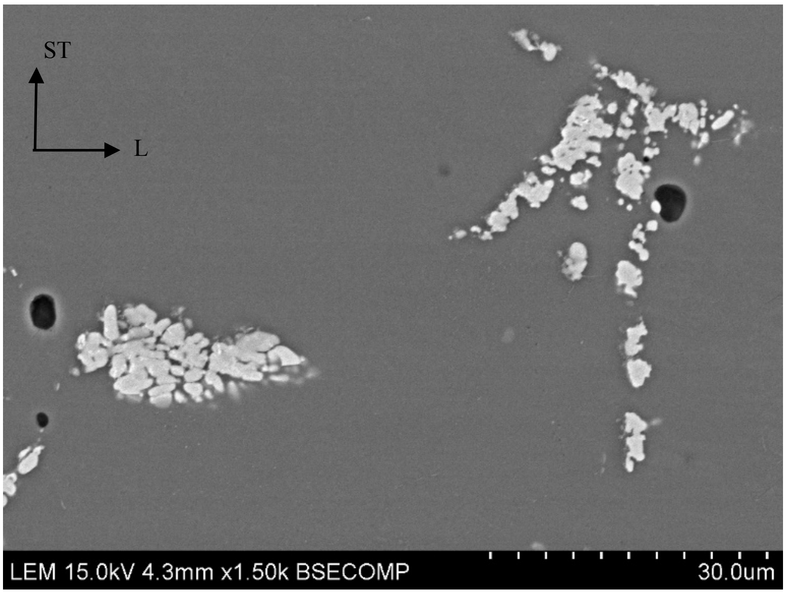

Figure 20. SEM detail of the area near the surface

DOI: 10.13009/EUCASS2019-603

A topography observation has been performed in figure 21, in order to identify in more detail, the constitution of these particles.

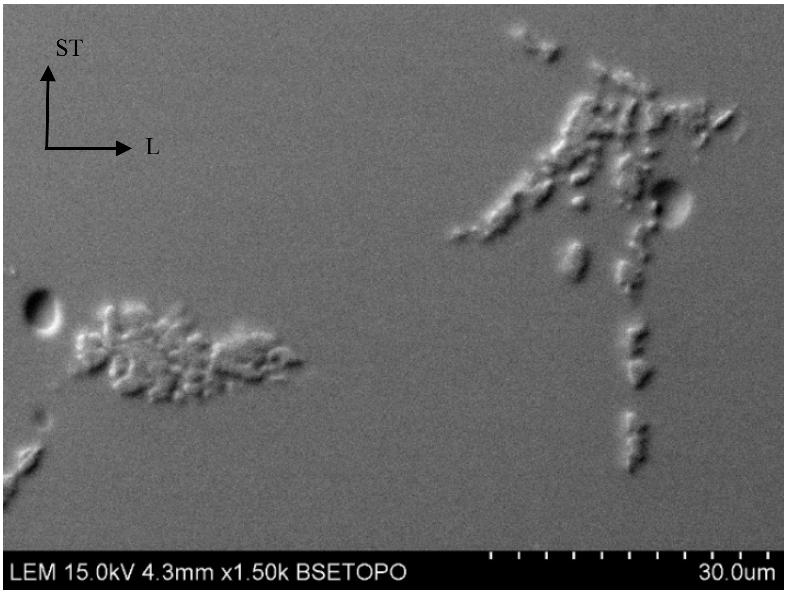

Figure 21. SEM detailed topography of the area near the surface.

Figure 20 confirms the polygonal and fragmented aspect of bright particles and the globular aspect of dark particles. Figure 21 shows that bright particles are apparently in relief and the dark particles are sunken. This micrograph suggests that bright particles are harder than dark particles.
The analysis of the figure 21 also suggests, that dark particles may be porosity which could have been filled during the last polishing operation with colloidal silica. In order to confirm the previous approaches, EDS analysis has been performed at the bright and dark intermetallic particles. EDS spectrums are shown in the figures 22 and 23.

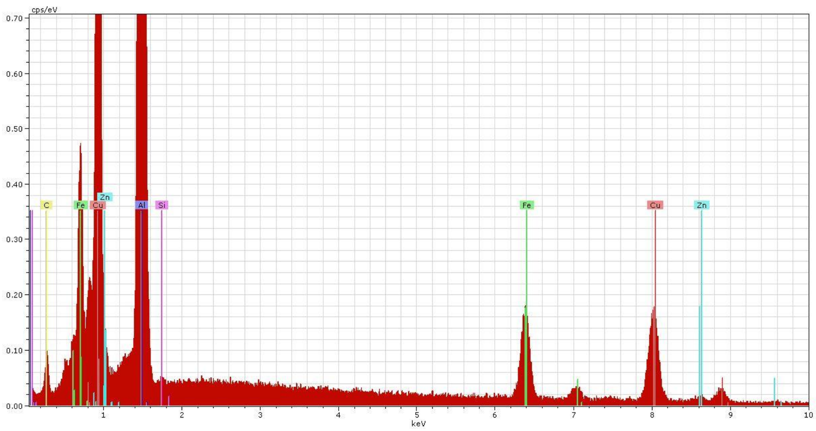

Figure 22. EDS spectrum for bright particles

DOI: 10.13009/EUCASS2019-603

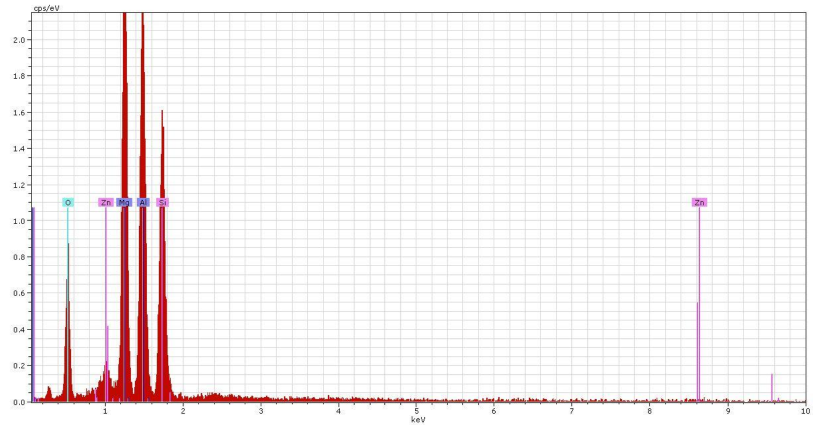

Figure 23. EDS spectrum for dark particles

Regarding the above EDS spectrums, the chemical compositions, in weight percentage for bright and dark particles, are shown in tables 6 and 7:

Table 6: EDS spectrums for bright particles (weight %)

Al	**Cu**	**Zn**	**Fe**	**Si**
49.4	33.8	3.8	13.0	0.1

Table 7: EDS spectrums for dark particles (weight %)

Al	**Mg**	**Zn**	**O**	**Si**
26.9	24.4	6.2	20.4	22.2

The chemical composition presented in tables 6 and 7 shows that bright particles are intermetallic compounds formed by Al, Cu, and Fe. This type of particles and their chemical composition match with [23] and [26]. The presence of Cu and Fe provides these particles with their bright colour. In addition, its chemical composition makes these particles hard and fragile. This is the main reason why bright particles are fragmented and oriented during rolling operations, according to figure 20, and appear in relief in figure 21.

Figure 14 shows that the number of bright particles near the surface is higher than in the centre of the plate. In addition, figures 16 and 17 show that the number of bright particles is much greater than the number of dark particles. Taking into account the chemical composition of the bright particles, table 6, this may explain that hardness near the surface is higher (174 HV30) that hardness in the centre of the plate (165 HV30). These hardness values have been measured in the as-received T7651 condition.

Regarding dark particles, EDS chemical composition shows that principal elements are Si and Mg with Al and high amount of Oxygen. The rounded shape and the fact that according to figure 21, these particles are sunken respect matrix, point them out as microcavities. Considering that the last operation of the metallographic preparation for the samples analysed by SEM and EDS has consisted in one polishing by colloidal silica, it may be possible that the microcavities have been partially filled by Oxygen and Si. This type of microcavities has been found in 7050 in proximity of polygonal intermetallic phase [23]. In any case, figure 21 also suggests that dark particles are less hardness that bright particles. But considering that the quantity of dark particles is considerably lower than that of bright particles, see figures 16 and 17, the impact into the global hardness due to presence of dark particles, is negligible.

DOI: 10.13009/EUCASS2019-603

4. Conclusions

- Tensile and yield (0.2%) strength, have been measured in longitudinal direction, L, through plate thickness in the as received conditions. The results obtained, are contrary to the expected ones, because tensile and yield (0.2%) strength are higher in the centre of the plate than near of the surface. The same behaviour has also been observed with other heat treatments, like for example peak aged (TT6), T7651 plus heating 160ºC for 8 hours treatment with a high over aged condition (TT10), interrupted aging treatment (T6I6), etc.

- A metallographic analysis, in the as-received T7651 condition, has been launched, in order to try to explain the un-expected mechanical strength properties measured.

- Grain deformed structure, observed by optical microscope, shows more deformed structure in the external surface than in the centre surface of the plate. This is a typical grain deformed shape structure.

- SEM observation shows two different kinds of intermetallic particles: ones in bright colour and other in dark colour.

-Finally, EDS semiquantitative microanalysis, shows no chemical segregation through the plate thickness, allowing for the characterization of the intermetallic particles observed by SEM.

-The conclusion of this first investigation is the microstructure observation does not permit to explain the un-expected measured values of tensile and yield strength properties.

In order to try to explain the abnormal variation, the following tests are been launched:

- Differential scanning calorimetry (DSC) analysis.
- Evaluation of the residual stress.
- Evaluation of the texture by electron backscatter diffraction (EBSD) technique.

DOI: 10.13009/EUCASS2019-603

References

[1] Dursun, T, & Soutis, C. Recent developments in advanced aircraft aluminium alloys. Materials and design (1980-2015) 56, 862-871.
[2] Starke, E.A & Staley, J.T (2011). Application of modern aluminium alloys to aircraft. In Fundamentals of Aluminium metallurgy (pp 747-783).
[3] I.J. Polmear. Recent developments in light alloys. Materials Transactions JIM Vol 37 Nº1 (pp 12 to 31)
[4] Mukhopadhyay, A.K, Reddy, G.M, Prasad, K.S, Varma, V.K & Mondal, C (2004). Microstructure property relationships in a high strength Al-Zn-Mg-Cu-Zr alloy. In materials Forum (Vol 28 pp883-888).
[5] Zheng, Z. Q., Zhong, S., Li, J. F, & Li, S, C (2012). Research on the high-cycle fatigue and crack initiation behaviour of AA7449 alloy. In /CAA13 Pittsburgh (pp 599-605). Springer, Cham.
[6] Rometsch, P.A., Zhang, Y., & Knight, S. (2014). Heat treatment of 7xxx series aluminium alloys- Some recent developments. Transactions of Nonferrous Metals society of China, 24(7), 2003-2017.
[7] Robinson, J. S., & Higgins, G. (2014). The influence of quenching and aging on fracture toughness of the Al-Zn-Mg-Cu alloy 7449. Materials Performance and Characterization, 3 (3) 370-388.
[8] Robinson. J. S., Tanner. D. A., Van Petegem. S. & Evans. A (2012). Influence of quenching and aging on residual stress in Al-Zn-Mg-Cu alloy 7449. Materials Science and Technology 28 (4) 420-430.
[9] Fribourg, G. (2009). Precipitation and plasticity couplings in a 7xxx aluminium alloy: application to thermomechanical treatments for distortion correction of aerospace component (Doctoral dissertation, Institute National Polytechnique of Grenoble- INPG).
[10] Kamp, N., Sinclair, I., & Starink, M. J (2002). Toughness-strength relations in the overaged 7449 Al-based alloy. Metallurgical and Materials Transactions A, 33(4), 1125-1136.
[11] Lequeu, P., Lassince, P., & Warner, T. (2007). Aluminium alloy development: For the airbus A380- Part 2. Advanced materials & processes, 165(7), 41-44.
[12] Aluminum Association (1984). Aluminum: properties and physical metallurgy. ASM international. John E. Hatch.
[13] ASM Specialty handbook, Aluminium and aluminium alloy. Edited by Joseph R. David (1993).
[14] Antoranz Perez, J.M (2012). Desarrollo de nuevos tratamientos térmicos para aleaciones avanzadas de interés aeroespacial. (Doctoral dissertation). Escuela Técnica superior de Ingenieros Aeronaúticos. Universidad Politécnica de Madrid
[15] ASM, H. (2004). Committee, ASM Metals Handbook Vol 9: Metallography and Microstructures.
[16] Birbilis, N., & Buchheit, R. G. (2005). Electrochemical characteristics of intermetallic phases in aluminium alloys an experimental survey and discussion. Journal of The Electrochemical Society, 152(4), B140-B151.
[17]https://businessdocbox.com/Metals/75177467-Thin-products-75-mm-7055-t7751-strength-mpa-500-thick-products-mm-year-first-used-in-aircraft.html
[18] Lumley, R .N.; Polmear, I. J.; Morton, A. H. Heat treatment of age-hardenable aluminium alloys: US, 7025839 B2.
[19] Buha, J., Lumley, R. N., & Crosky, A. G. (2006). Microstructural development and mechanical properties of interrupted aged Al-Mg-Si-Cu alloy. Metallurgical and Materials Transactions A, 37 (10), 3119-3130.
[20] UNE-EN-ISO 6892-1:2009. Materiales metálicos. Ensayo de tracción. Parte 1: Método de ensayo a temperatura ambiente.
[21] Xu, D. K., Rometsch, P. A., & Birbilis, N. (2012). Improved solution treatment for and as-rolled Al-Zn-Mg-Cu alloy. Part I. Characterisation of constituent particles and overheating. Materials science and Engineering: A, 534, 234-243.
[22] Xu, D. K., Rometsch, P. A., & Birbilis, N. (2012). Improved solution treatment for and as-rolled Al-Zn-Mg-Cu alloy. Part II. Microstructure and mechanical properties. Materials science and Engineering: A, 534, 244-252.
[23] Brotzu, A., De Lellis, G., Felli, F., & Pilone, D. (2017). Study of defect formation in Al 7050 alloys. Procedia structural integrity. 3, 246-252
[24] Han, N. M., Zhang, X. M., Liu, S. D., He, D. G. & Zhang, R. (2011). Effect of solution treatment on the strength and fracture toughness of aluminium alloy 7050. Journal of alloys and compounds, 509 (10), 4138-4145.
[25] Dumont, D., Deschamps, A. & Brechet, Y. (2003). On the relationship between microstructure, strength, and toughness in AA 7050 aluminium alloy. Materials Science and Engineering: A, 356 (1-2), 326-336.
[26] Birbilis, N., Cavanaugh, M. K., Buchheit, R. G., Harlow, D. G. &Wei, R. (2005). Symposium Applications of materials science to military systems. Materials Science and Technology, 5. Pisttsburgh, PA.